

Range Cell Migration Correction for Phase Error Compensation of Highly Squinted SAR

Minh Phuong Nguyen, Leibniz Universität Hannover, nguyenmp@tnt.uni-hannover.de, Germany

Abstract

Phase error compensation within motion compensation techniques requires range cell migration corrected SAR data. The main contribution of this paper is providing a non-approximated range cell migration correction (RCMC) for processing highly squinted SAR data. Embedded in the conventional Omega-K processing, the approach consists of two coordinate transformations carried out in the 2D frequency domain and a modification made to the 2D matched filter. The first coordinate transformation is a rotation that removes the effect of the squint angle, the second one is an azimuth wavenumber dependent shift of the range wavenumber. It is shown that the proposed approach works for squint angles up to 60° .

1 Introduction

Airborne SAR systems are disturbed by motion errors, which – if not corrected – lead to image quality degradation. By recording the relevant motion parameters with an on-board GPS/IMU system, the real movement of the sensor can be taken into account by motion compensation (MoCom) techniques. Common MoCom procedure consists of a first order MoCom and a residual/second order MoCom, of which the latter requires a range cell migration correction (RCMC) of the SAR data [1, 2].

For squinted spotlight SAR, the Omega-K processor is suitable to deal with long azimuth illumination time and high squint angle. In contrast to other SAR processors in the frequency domain, the Omega-K algorithm does not use any approximations and attains almost the ultimate resolution of the SAR image [3]. However, an approach to accomplish RCMC explicitly within the Omega-K algorithm for the general case of high squint angle has not been described so far.

Reigber et al. [1] developed an extended Omega-K algorithm with integrated MoCom where RCMC is realized by a modified Stolt mapping. This approach provides good results for broadside SAR with small squint angle. A RCMC approach for squinted SAR is described by Cumming and Wong [4]. However, the derivation of this RCMC involves in some approximations, resulting in the fact that this method works only well for squint angles up to 20° .

In this paper a method to achieve RCMC without approximations for the case of high squint angle will be derived. The RCMC is embedded in the Omega-K algorithm. A high squint angle causes a strong coupling of the azimuth and range frequency, which makes RCMC difficult. Hence, the squint angle is the main obstacle for RCMC and therefore has to be compensated. Since the squint angle induces a rotation of the SAR data spectrum, its effect can be eliminated by a coordinate transformation in the 2D frequency domain. After the coordinate rotation, modified Stolt mapping can be applied to realize

RCMC.

In the next section the signal model for SAR data taken in squinted spotlight mode is described. The conventional Omega-K algorithm for squinted SAR is revised in section 3. Afterwards, section 4 presents the modifications made to the Omega-K processing to achieve RCMC. Results and discussions are presented in section 5.

2 Signal model of squinted spotlight SAR

While the platform moves with a constant velocity v along the azimuth x -axis, the radar illuminates the ground within $[-L/2, L/2]$, see Fig. 1. The slant range r is perpendicular to the x -axis. In the presence of the squint angle θ_s , the wave propagation direction \tilde{r} is rotated by θ_s from the slant range r .

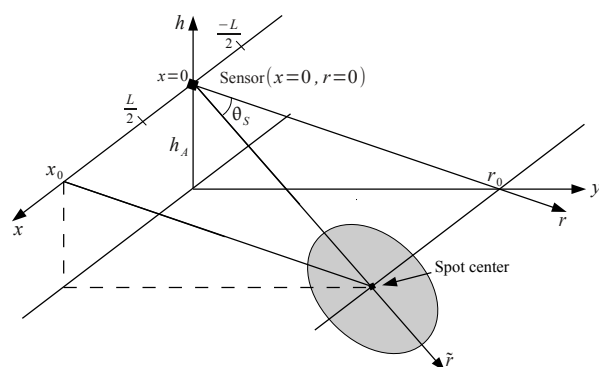


Figure 1: SAR geometry in squinted spotlight mode

The range compressed signal of a single point target \mathbf{p}_0 located at the spot center (x_0, r_0) with a reflectivity $\delta(x - x_0, r - r_0)$ can be written as [5]

$$d(x, t, \mathbf{p}_0) = p_r\{t\} * g(x, t) \quad (1)$$

with the impulse response of the SAR system

$$g(x, t) = \delta \left\{ t - \left(\frac{2R(x, \mathbf{p}_0)}{c} - t_0 \right) \right\} \cdot \exp \left\{ -j\omega_c \left(\frac{2R(x, \mathbf{p}_0)}{c} - t_0 \right) \right\}, \quad (2)$$

where c is the speed of light, ω_c the angular carrier frequency and $p_r\{\cdot\}$ the range pulse envelope. The distance $R(x, \mathbf{p}_0)$ depends on the position of the point target \mathbf{p}_0 and the actual position x of the sensor during the illumination time according to the range migration equation

$$R(x, \mathbf{p}_0) = \sqrt{(x - x_0)^2 + r_0^2}. \quad (3)$$

The reference time $t_0 = \frac{2\sqrt{x_0^2 + r_0^2}}{c}$ is chosen for normalization so that the reconstructed image of the point target lies at the origin of the SAR image.

The following 2D Fourier transform of the SAR system impulse response $g(x, t)$ is computed in two steps. First, the Fourier transform in range direction is calculated resulting in

$$G(x, \omega) = \exp \left\{ -j\omega \left(\frac{2R(x, \mathbf{p}_0)}{c} - t_0 \right) \right\}, \quad (4)$$

where $\omega = \omega' + \omega_c$ is the angular frequency modulated by ω_c . Second, the Fourier transform of (4) in azimuth direction can be calculated analytically by using the principle of stationary phase. A stationary point of the phase is given for

$$x = \frac{r_0 k_x}{\sqrt{\left(\frac{2\omega}{c}\right)^2 - k_x^2}} + x_0, \quad (5)$$

where $k_x = k'_x + k_{xc}$ with the azimuth center wavenumber $k_{xc} = 4\pi \sin \theta_s / \lambda$, yielding the transfer function of the SAR system

$$G(k_x, \omega) = \exp \left\{ j \left(\omega t_0 - r_0 \sqrt{\left(\frac{2\omega}{c}\right)^2 - k_x^2} - x_0 k_x \right) \right\}. \quad (6)$$

3 Omega-K processing

The inverse 2D Fourier transform of the product of the 2D data spectrum and a matched filter yields the focused SAR image $b(x', t')$, where $x' = x - x_0$ and $t' = t - t_0$ [3]. For a practical implementation, the base-band data spectrum $D_c(k'_x, \omega')$ is applied [3]

$$b(x', t') = \exp\{j(x' k_{xc} + t' \omega_c)\} \iint D_c(k'_x, \omega') \cdot H(k'_x + k_{xc}, \omega' + \omega_c) \cdot \exp\{j(k'_x x' + \omega' t')\} dk'_x d\omega', \quad (7)$$

where $H(k_x, \omega)$ is the complex conjugate of $G(k_x, \omega)$ in (6). The exponential term outside of the integral (7) corresponds to the shift by k_{xc} and ω_c of the base-band spectrum $D_c(k'_x, \omega')$ to $D(k_x, \omega)$ in the high frequency domain.

Furthermore, it is desired to have the focused SAR image in spatial coordinates (x, r) . After the Stolt mapping according to

$$\omega \rightarrow k_r = \sqrt{\left(\frac{2\omega}{c}\right)^2 - k_x^2}, \quad (8)$$

the desired focused SAR image is

$$b(x', r') = \exp\{j(x' k_{xc} + r' k_{rc})\} \iint D_c(k'_x, k'_r) \cdot H(k'_x + k_{xc}, k'_r + k_{rc}) \frac{c|k'_r + k_{rc}|}{2\sqrt{(k'_x + k_{xc})^2 + (k'_r + k_{rc})^2}} \cdot \exp\{j(k'_x x' + k'_r r')\} dk'_x dk'_r, \quad (9)$$

where $r' = r - r_0$ and $k'_r = k_r - k_{rc}$ with

$$k_{rc} = \sqrt{\left(\frac{2\omega_c}{c}\right)^2 - k_{xc}^2}.$$

In summary, the Omega-K algorithm first performs a 2D Fourier transform of the quadrature demodulated, range compressed and Doppler shift corrected SAR data. The Stolt mapping then performs the change of variables (8). Subsequently, the 2D spectrum $D_c(k'_x, k'_r)$ is multiplied by the 2D matched filter

$$H(k_x, k_r) = \exp \left\{ -j \left(\frac{ct_0}{2} \sqrt{k_x^2 + k_r^2} - r_0 k_r - x_0 k_x \right) \right\}. \quad (10)$$

The obliquity factor $\frac{|k_r|}{\sqrt{k_x^2 + k_r^2}}$ is approximately a constant due to the small relative bandwidth of k_x [3]. Finally, the 2D inverse Fourier transform yields the desired SAR image of the illuminated area centered at (x_0, r_0) .

For further analysis, the 2D filter (10) can be rewritten in dependence on the squint angle θ_s as

$$H(k_x, k_r) = \exp \left\{ -j \sqrt{x_0^2 + r_0^2} \left(\sqrt{k_x^2 + k_r^2} - \cos \theta_s k_r - \sin \theta_s k_x \right) \right\} \quad (11)$$

with $\sin \theta_s = \frac{x_0}{\sqrt{x_0^2 + r_0^2}}$ and $\cos \theta_s = \frac{r_0}{\sqrt{x_0^2 + r_0^2}}$.

4 Range cell migration correction in Omega-K processing

After transforming the range compressed SAR data into the 2D frequency domain and performing Stolt mapping, RCMC is realized in two steps described in subsections 4.1 and 4.2.

4.1 Rotation by θ_s

Fig. 2 (a) and (b) show the SAR data spectrum before and after the Stolt mapping. In particular, Fig. 2 (b) indicates the rotation of the spectrum by the squint angle θ_s . Hence, the effect of the squint angle can be removed by a coordinate transformation that compensates this rotation. The coordinate transformation of the SAR spectrum is carried out in the 2D frequency domain according to

$$\begin{pmatrix} \tilde{k}_x \\ \tilde{k}_r \end{pmatrix} = \begin{pmatrix} \cos \theta_s & -\sin \theta_s \\ \sin \theta_s & \cos \theta_s \end{pmatrix} \cdot \begin{pmatrix} k_x \\ k_r \end{pmatrix}. \quad (12)$$

The SAR spectrum $D(\tilde{k}_x, \tilde{k}_r)$ can be calculated by two 1D interpolations [6]. The focused SAR image in the accordingly rotated spatial coordinates ($\tilde{x}, \tilde{r} = \tilde{r}' + \tilde{r}_0$) (squinted azimuth and squinted range) is

$$b(\tilde{x}, \tilde{r}') = \exp\{-j\tilde{r}'k_c\} \iint D_c(\tilde{k}_x, \tilde{k}_r') \cdot H(\tilde{k}_x, \tilde{k}_r' + k_c) \cdot \exp\left\{j\left(\tilde{k}_x\tilde{x} + \tilde{k}_r'\tilde{r}'\right)\right\} d\tilde{k}_x d\tilde{k}_r'. \quad (13)$$

Note that the relationship $k_x^2 + k_r^2 = \tilde{k}_x^2 + \tilde{k}_r^2$ with $\tilde{k}_r = \tilde{k}_r' + k_c$ is held. The rotation $(x, r) \rightarrow (\tilde{x}, \tilde{r})$ in space domain by θ_s yields $\tilde{r}_0 = \sqrt{x_0^2 + r_0^2}$ and $\tilde{x}_0 = 0$. The 2D filter (11) changes to

$$H(\tilde{k}_x, \tilde{k}_r) = \exp\left\{-j\tilde{r}_0\left(\sqrt{\tilde{k}_x^2 + \tilde{k}_r^2} - \tilde{k}_r\right)\right\}. \quad (14)$$

Comparison between (11) and (14) shows that the rotation (12) in the 2D frequency domain removes the effect of the squint angle completely, see also Fig. 2 (c). In the new coordinate system (\tilde{x}, \tilde{r}) , the effective squint angle is zero.

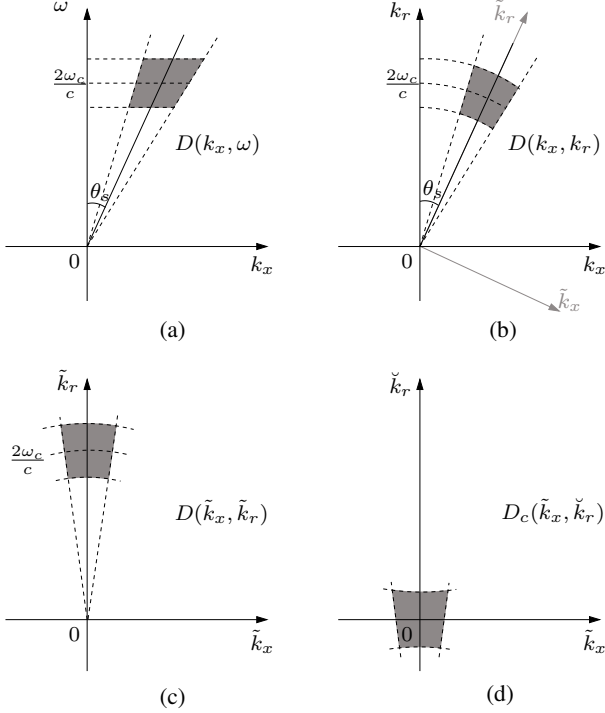


Figure 2: SAR data spectrum (a) of the acquired data, (b) after Stolt mapping, (c) after 2D rotation and (d) after shifting in \tilde{k}_r -direction

4.2 Shift by $\sqrt{k_c^2 - \tilde{k}_x^2}$

In order to allow RCMC a substitution of variables

$$\tilde{k}_r \rightarrow \check{k}_r = \tilde{k}_r - \sqrt{k_c^2 - \tilde{k}_x^2}, \quad (15)$$

is applied, which was first introduced by Reigber et al. [1], where $k_c = \frac{2\omega_c}{c}$ is the wavenumber at carrier frequency. This coordinate transformation corresponds to a

shift of the data spectrum in the direction of the range wavenumber. The equation (15) causes all data points referring to k_c to be mapped to a line with constant $\check{k}_r = 0$ (see Fig. 2 (d)). With the shifted spectrum $D_c(\tilde{k}_x, \check{k}_r)$, the focused SAR image is calculated as

$$b(\tilde{x}, \tilde{r}') = \int \exp\left\{j(\tilde{r}' + \tilde{r}_0)\sqrt{k_c^2 - \tilde{k}_x^2}\right\} \cdot \int D_c(\tilde{k}_x, \check{k}_r) \cdot H_{mod}(\tilde{k}_x, \check{k}_r) \cdot \exp\left\{j\left(\tilde{k}_x\tilde{x} + \check{k}_r\tilde{r}'\right)\right\} d\check{k}_r d\tilde{k}_x \quad (16)$$

with

$$H_{rcmc}(\tilde{k}_x, \check{k}_r) = \exp\left\{-j\tilde{r}_0\left(\sqrt{\tilde{k}_x^2 + \left(\check{k}_r + \sqrt{k_c^2 - \tilde{k}_x^2}\right)^2} - \check{k}_r\right)\right\}. \quad (17)$$

Note that the first exponential term in (16)

$$H_{az}(\tilde{k}_x, \tilde{r}) = \exp\left\{j\tilde{r}\sqrt{k_c^2 - \tilde{k}_x^2}\right\} \quad (18)$$

is an azimuth filter that only depends on \tilde{r} and \tilde{k}_x . This term is responsible for the final azimuth focusing of the SAR data after RCMC.

In summary, the flowchart in Fig. 3 shows the necessary steps for RCMC within the Omega-K algorithm.

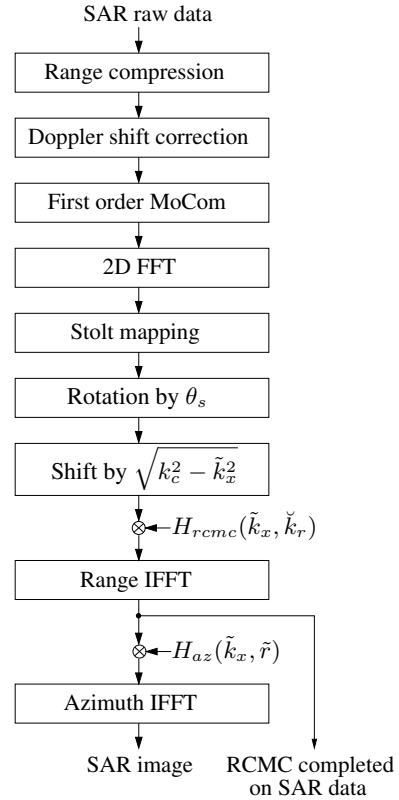


Figure 3: SAR focusing with the proposed method. Phase error compensation can be applied on the SAR data after RCMC.

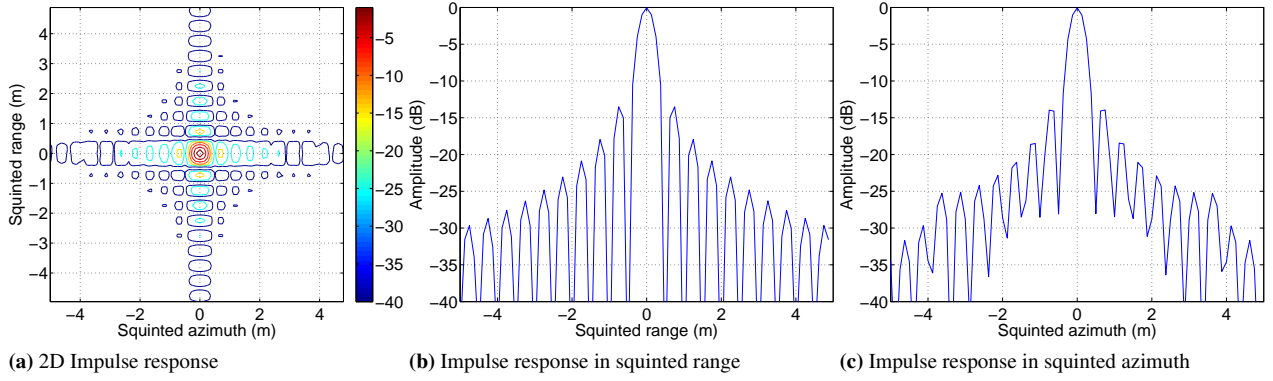


Figure 4: Simulation results for $\theta_s = 60^\circ$.

5 Results

Fig. 4 presents the results of X-band SAR simulations with parameters shown in Table 1. Targets are distributed in a region with a reference range $\tilde{r}_0 = 16$ km and a squint angle $\theta_s = 60^\circ$. SAR raw data were simulated and processed with the proposed method. No window function for sidelobe suppression is applied.

The extent of the SAR data after RCMC in (\tilde{x}, \tilde{r}) is skewed to length of $\tilde{L} = L \cdot \cos \theta_s$. This fact has to be considered when applying residual phase error compensation within adequate second order MoCom [2]. The residual phase error with a length of L calculated in the (x, r) -coordinates then has to be skewed by the factor of $\cos \theta_s$ to fit the SAR data after RCMC.

Fig. 4 (a) shows the focusing result of a point target in the rotated coordinates (\tilde{x}, \tilde{r}) . As expected, the sidelobes are orientated parallel to the axes as in the non-squinted case. In Fig. 4 (b) and (c), the profiles of the impulse responses in squinted range and squinted azimuth are close to the ideal sinc-function.

Table 1: Simulation parameters

Carrier frequency f_c	10 GHz
Pulse bandwidth B_p	300 MHz
Pulse duration T	6 μ s
Sample frequency	360 MHz
Platform velocity v	100 m/s
Synthetic aperture length L	1000 m
Pulse repetition frequency	800 Hz

6 Conclusions

A non-approximated RCMC for highly squinted SAR imaging is presented in this paper. The proposed method is conveniently embedded in the Omega-K algorithm, which itself works without approximations. With the proposed RCMC, second order MoCom can be easily applied to compensate residual phase error. In doing so, the

extent of the original phase error has to be skewed to fit the SAR data in the rotated space domain.

The only limitation of the proposed method is that it needs a 2D interpolation, which means one 1D interpolation more than the conventional Omega-K algorithm. This additional 1D interpolation results in higher computational effort. On the contrary, the final SAR image is rotated by the squint angle so that the sidelobes of point reflectors are parallel to the axes. This way of data representation is practical for point target analysis like PSLR or ISLR calculations.

References

- [1] A. Reigber, E. Alivizatos, A. Potsis and A. Moreira: *Extended Wavenumber-Domain Synthetic Aperture Radar Focusing with Integrated Motion Compensation*, IEE Proc.-Radar Sonar Navig., Vol. 153, No. 3, pp. 301–310, June 2006.
- [2] M. P. Nguyen and S. Ben Ammar: *Second Order Motion Compensation for Squinted Spotlight Synthetic Aperture Radar*, Proc. Asia-Pacific Conference on Synthetic Aperture Radar (APSAR), pp. 202–205, 2013.
- [3] C. Cafforio, C. Prati and F. Rocca: *SAR data focusing using seismic migration techniques*, IEEE Transaction on Aerospace and Electronic Systems, pp. 194–207, March 1991.
- [4] I. G. Cumming and F. H. Wong: *Digital Signal Processing of Synthetic Aperture Radar: Algorithms and Implementation*, pp. 250–256, Artech House, 2005.
- [5] R. Bamler: *A Comparison of Range-Doppler and Wavenumber Domain SAR Focusing Algorithms*, IEEE Transactions on Geoscience and Remote Sensing, Vol. 30, No. 4, pp. 706–713, 1992.
- [6] K.-T. Kim, J.-I. Park and S.-H. Park: *Motion Compensation for Squint Mode Spotlight SAR Imaging using Efficient 2D Interpolation*, Progress In Electromagn. Research, Vol. 128, pp. 503–518, 2012.